

## Turbulent Transport in Tokamak Plasmas with Rotational Shear

M. Barnes,<sup>1,2,\*</sup> F. I. Parra,<sup>1</sup> E. G. Highcock,<sup>1,2</sup> A. A. Schekochihin,<sup>1</sup> S. C. Cowley,<sup>2</sup> and C. M. Roach<sup>2</sup>

<sup>1</sup>*Rudolf Peierls Centre for Theoretical Physics, University of Oxford, Oxford OX1 3NP, United Kingdom*

<sup>2</sup>*Euratom/CCFE Fusion Association, Culham Science Centre, Abingdon OX14 3DB, United Kingdom*

(Received 20 July 2010; published 29 April 2011)

Nonlinear gyrokinetic simulations are conducted to investigate turbulent transport in tokamak plasmas with rotational shear. At sufficiently large flow shears, linear instabilities are suppressed, but transiently growing modes drive subcritical turbulence whose amplitude increases with flow shear. This leads to a local minimum in the heat flux, indicating an optimal  $\mathbf{E} \times \mathbf{B}$  shear value for plasma confinement. Local maxima in the momentum fluxes are observed, implying the possibility of bifurcations in the  $\mathbf{E} \times \mathbf{B}$  shear. The critical temperature gradient for the onset of turbulence increases with flow shear at low flow shears; at higher flow shears, the dependence of heat flux on temperature gradient becomes less stiff. The turbulent Prandtl number is found to be largely independent of temperature and flow gradients, with a value close to unity.

DOI: 10.1103/PhysRevLett.106.175004

PACS numbers: 52.55.-s, 52.30.Gz, 52.35.Ra, 52.65.-y

*Introduction.*—Experimental measurements in magnetic confinement fusion devices indicate that sheared mean  $\mathbf{E} \times \mathbf{B}$  flows can significantly reduce and sometimes fully suppress turbulent particle, momentum, and heat fluxes [1,2]. Since these fluxes determine mean plasma density and temperature profiles, their reduction leads to a local increase in the profile gradients. This increase can be dramatic: transport barriers in both the plasma core and edge have been measured with radial extents of only tens of ion Larmor radii [3]. The associated increase in core density and temperature results in increased fusion power. Thus, understanding how shear flow layers develop and what effect they have on turbulent fluxes is both physically interesting and practically useful.

This Letter reports a numerical study of the influence of sheared toroidal rotation on turbulent heat and momentum transport in tokamak plasmas. Two main effects of sheared rotation were identified in previous numerical work [4–9]: suppression of turbulent transport by shear in the perpendicular (to the mean magnetic field) velocity and linear destabilization due to the parallel velocity gradient (PVG). While the former observation indicates that a finite flow shear improves plasma confinement, the latter raises the question of whether more shear is always beneficial. Prior simulation results with low to moderate flow shear indicated that the PVG linear growth rate increases monotonically with flow shear [6,9]. Below we report that the PVG-driven linear instability [10] is stabilized at larger flow shear values, leading to a dip in the heat flux. However, transiently growing modes driven by the PVG eventually give rise to subcritical turbulence for sufficiently large flow shear. The fluxes associated with this subcritical turbulence increase with flow shear, leading to an optimal value of flow shear for each temperature gradient comparable to that found in many experimental transport barriers [11].

In the absence of flow shear, a small increase in temperature gradient leads to a large increase in heat flux (“stiff transport”). Recent experimental evidence [12] suggests that flow shear may reduce this sensitivity in configurations with low magnetic shear. Our results indicate that at low flow shears, both the critical temperature gradient for the onset of turbulence and the stiffness increase. At high flow shears, the opposite behavior is observed (stiffness and critical temperature gradient both decrease).

*Model.*—A closed set of fluid conservation equations determines the evolution of mean plasma density, flow, and pressure in tokamak plasmas [13,14]. The fluxes appearing in these equations are typically dominated by turbulent contributions, which we calculate here. We restrict our attention to electrostatic fluctuations and assume a modified Boltzmann response [15] for the electron distribution. The particle flux then vanishes, and the radial components of the turbulent heat flux of species  $s$ ,  $Q_s$ , and toroidal angular momentum flux,  $\Pi$ , are

$$Q_s = \overline{\int d^3\mathbf{v} \left( \frac{m_s v^2}{2} \right) \left( \mathbf{v}_E \cdot \frac{\nabla\psi}{|\nabla\psi|} \right) \delta f_s}, \quad (1)$$

$$\Pi = \sum_s m_s R^2 \overline{\int d^3\mathbf{v} (\mathbf{v} \cdot \nabla\phi) \left( \mathbf{v}_E \cdot \frac{\nabla\psi}{|\nabla\psi|} \right) \delta f_s}, \quad (2)$$

with  $R$  the major radius of the torus,  $\psi$  a flux-surface label,  $\phi$  the toroidal angle,  $m_s$  the particle mass,  $\mathbf{v}$  its velocity in the mean flow frame,  $\mathbf{v}_E$  the fluctuating  $\mathbf{E} \times \mathbf{B}$  drift velocity,  $\delta f_s$  the deviation of the distribution function from a local Maxwellian, and the overline a spatial average over a thin annulus encompassing a flux surface.

The distribution function  $\delta f_s$  is calculated by solving the standard  $\delta f$  gyrokinetic equation in the limit where the plasma flow speed,  $u$ , is ordered comparable to the ion

thermal speed,  $v_{th} \equiv \sqrt{T/m}$ , with  $T$  the species temperature [14,16]. In this “high-flow” regime, the flow velocity is constrained to be  $\mathbf{u} = R^2\omega(\psi)\nabla\phi$ , where  $\omega$  is the rotational frequency [17]. To focus on the effect of flow shear, we consider the limit in which the flow is small, but the flow shear is large (comparable to the fluctuation frequency). We thus ignore effects arising from the centrifugal and Coriolis forces. Using  $(\mathbf{R}, E, \mu, \vartheta)$  coordinates, with  $\mathbf{R}$  the guiding center position,  $E = mv^2/2$ ,  $\mu = mv_{\perp}^2/2B$ , and  $\vartheta$  the gyro angle, the gyrokinetic equation is

$$\begin{aligned} & \frac{d\langle\delta f\rangle}{dt} + (\mathbf{v}_{\parallel}\hat{\mathbf{b}} + \mathbf{v}_B + \langle\mathbf{v}_E\rangle) \cdot \nabla \left( \langle\delta f\rangle + \frac{e\langle\varphi\rangle}{T}F_0 \right) \\ & = \langle C[\delta f] \rangle - \langle\mathbf{v}_E\rangle \cdot \nabla\psi \left( \frac{\partial F_0}{\partial\psi} + \frac{mv_{\parallel}}{T} \frac{RB_{\phi}}{B} \frac{d\omega}{d\psi} F_0 \right), \end{aligned} \quad (3)$$

with  $d/dt = \partial/\partial t + \mathbf{u} \cdot \nabla$ ,  $e$  the particle charge,  $\varphi$  the electrostatic potential,  $\mathbf{v}_E = (c/B^2)\mathbf{B} \times \nabla\varphi$ ,  $F_0$  a Maxwellian distribution in the frame rotating with frequency  $\omega$ ,  $C$  the collision operator,  $B$  the magnetic field strength,  $B_{\phi}$  its toroidal component,  $\mathbf{v}_B = \hat{\mathbf{b}}/\Omega \times (v_{\parallel}^2\hat{\mathbf{b}} \cdot \nabla\hat{\mathbf{b}} + v_{\perp}^2\nabla B/2B)$ ,  $\Omega$  the Larmor frequency,  $\hat{\mathbf{b}} = \mathbf{B}/B$ , and  $\langle.\rangle$  the average over  $\vartheta$  at fixed  $(\mathbf{R}, E, \mu)$ .

Equation (3) is solved in the rotating reference frame using the local, nonlinear gyrokinetic code GS2 [18]. Flow shear enters the calculation through the convective time derivative, which depends on the shear in the perpendicular flow, and the  $d\omega/d\psi$  drive term in Eq. (3), which accounts for the shear in the parallel flow. Because the flow is purely toroidal, these two components are related by the geometric factor  $(qR_0/r)$  [9]. The flow shear is thus controlled by a single parameter,  $\gamma_E = (\psi/q)(d\omega/d\psi)R_0/\sqrt{2}v_{th} = (M/q)(d\ln\omega/d\ln r)$ , with  $q$  the safety factor,  $R_0$  the major radius at the center of the flux surface, and  $r$  the half-diameter of the flux surface (both measured at the height of the magnetic axis).

We study a system whose magnetic geometry corresponds to the widely used Cyclone base case [19] (unshifted, circular flux surface with  $q = 1.4$ , magnetic shear  $\hat{s} = d\ln q/d\ln r = 0.8$ ,  $r/R_0 = 0.18$ , and  $R_0/L_n = 2.2$ , where  $L_n^{-1} = -d\ln n/dr$ ). The shearing rate,  $\gamma_E$ , and the normalized inverse temperature gradient scale length,  $\kappa \equiv R_0/L_T$ , were varied over a wide range of values in a series of linear and nonlinear simulations.

*Linear stability.*—In tokamaks, mean  $\mathbf{E} \times \mathbf{B}$  shear advects fluctuations through regions where the magnetic field line curvature alternates between stabilizing and destabilizing. The resulting modes, called Floquet modes, exhibit periodic oscillations superposed on mean growth or decay (the time domain analog of Bloch states in periodic media). The mean linear growth rates,  $\gamma$ , obtained from our simulations are given in Fig. 1. We find that  $\gamma$  decreases discontinuously when  $\gamma_E$  increases from zero [20] before increasing to a local maximum and subsequently decreasing to zero. For  $\gamma_E \gtrsim 0.25$ , the system is linearly stable

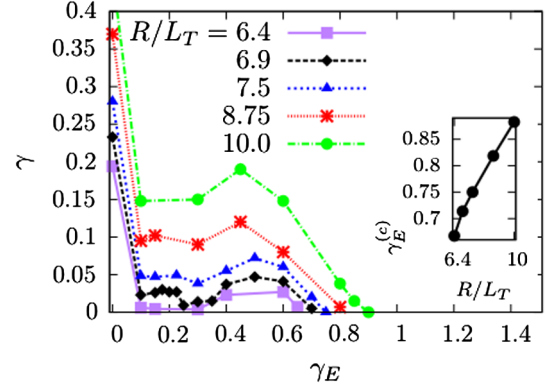


FIG. 1 (color online). Average linear growth rates (normalized by  $R_0/v_{th}$ ) vs flow shear. Inset: Critical flow shear vs  $R_0/L_T$ .

unless both the ion temperature gradient and the PVG are nonzero (cf. [6–9]). The system becomes linearly stable for larger values of  $\gamma_E$ , with the critical  $\gamma_E$  for stability,  $\gamma_{Ec}$ , increasing approximately linearly with  $\kappa$ . Beyond  $\gamma_{Ec}$ , there are no linearly unstable modes, which is similar to the result from fluid theory in a slab [21]. While  $\gamma_{Ec}$  is larger than the  $\gamma_E$  values found for standard operating conditions in many tokamaks, it is comparable to or smaller than the  $\gamma_E$  values observed in many transport barriers [11].

*Heat flux.*—The turbulent heat flux calculated from nonlinear simulations is given in Fig. 2. For all  $\kappa$  values, the heat flux follows the same trend as growth rates when  $\gamma_E < \gamma_{Ec}$ . For  $\gamma_E > \gamma_{Ec}$ , nonlinear simulations initialized with low-amplitude noise develop no turbulent transport. However, for finite initial fluctuation amplitudes, the turbulence does not necessarily decay away: for sufficiently large values of  $\kappa$  and initial amplitude, the flux reaches steady state values in excess of those found for  $\gamma_E$  just below  $\gamma_{Ec}$  [22]. The flux then increases monotonically with  $\gamma_E$ . For the range of  $\gamma_E$  considered here, the heat flux associated with a given temperature gradient is thus minimized at a finite value of flow shear.

*Subcritical turbulence.*—Because the turbulence is present in the absence of linear instability, we refer to it as subcritical. When  $\gamma_E > \gamma_{Ec}$ , our linear simulations exhibit transient growth, with order unity increases in the initial fluctuation amplitudes over times of several  $R_0/v_{th}$  before subsequent decay (Fig. 3). The duration of growth decreases with increasing  $\gamma_E$ , but the transient growth rate increases so that the amplification factor of the initial perturbation amplitude grows with flow shear, consistent with analytic theory [21]. This provides an energy source for the turbulence, which can be maintained by the nonlinearity through redistribution of energy among other modes. As seen in Fig. 2, the  $\gamma_E$  beyond which subcritical turbulence is maintained depends on  $\kappa$  (and likely on magnetic geometry as well).

The phenomenon reported here is physically distinct from the subcritical turbulence observed previously (cf. [6]), which is sustained by the transient growth of

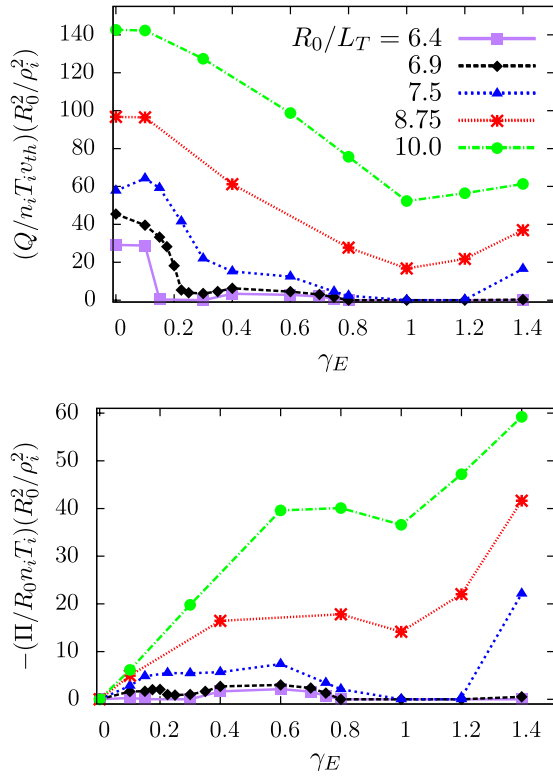


FIG. 2 (color online). Turbulent heat (top) and toroidal angular momentum (bottom) fluxes vs flow shear for a range of  $R_0/L_T$  values. For  $\gamma_E > \gamma_{Ec}$  (see Fig. 1), the turbulence is subcritical, sustained by transiently growing modes.

Floquet oscillations as modes are advected through the unfavorable curvature region by the  $\mathbf{E} \times \mathbf{B}$  flow. The subcritical turbulence presented here is driven by the PVG term in Eq. (3) ( $d\omega/d\psi$  term on the right-hand side), as the turbulence disappears when the PVG is artificially set to zero; thus, it is present even for a straight magnetic field. This is physically similar to subcritical turbulence in Couette and Poiseuille flows, where strong flows drive

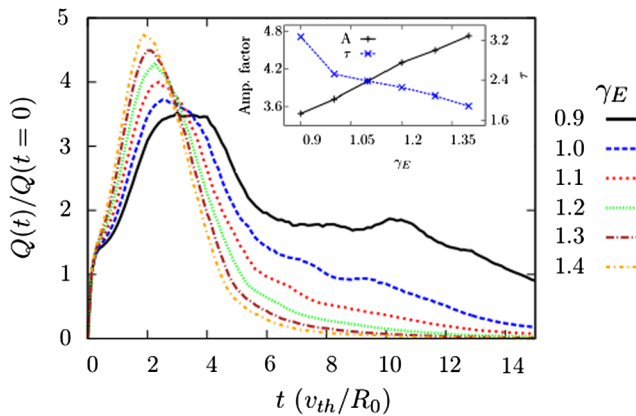


FIG. 3 (color online). Heat flux versus time obtained from linear simulations for  $R_0/L_T = 8.75$  and several  $\gamma_E$  values at which subcritical turbulence is observed. Inset: Transient amplification factor,  $A$ , and growth time,  $\tau$ , versus  $\gamma_E$ .

turbulence in the absence of linear (and nonlinear) instabilities [23].

*Momentum flux.*—The momentum flux also mimics the linear growth rate, except near  $\gamma_E = 0$  [24]. This is understood by expressing the momentum flux as  $\Pi = -m_i v_{th}(qR_0/r)v_i(\kappa, \gamma_E)\gamma_E$ , where  $v_i$  is the turbulent viscosity. For small  $\gamma_E$ ,  $v_i$  is approximately constant and  $\Pi \propto \gamma_E$ . For larger  $\gamma_E$ , turbulent amplitudes drop rapidly, so  $\Pi$  decreases, resulting in the local maxima seen in Fig. 2. This suppression of  $\Pi$  is due to linear stabilization as  $\gamma_E$  approaches  $\gamma_{Ec}$  from below. The momentum flux increases monotonically when  $\gamma_E > \gamma_{Ec}$  due to subcritical turbulence. The maxima in  $\Pi$  may lead to a bifurcation in flow shear, discussed in the Conclusions.

*Prandtl number.*—The turbulent Prandtl number can be calculated from the values of  $Q_i$  and  $\Pi$ . It is defined as  $Pr = v_i/\chi_i$ , where the turbulent thermal diffusivity,  $\chi_i$ , is given by  $Q_i = -\chi_i dT_i/dr$ . Figure 4 shows that  $Pr$  is approximately independent of  $\kappa$  and only has strong dependence on  $\gamma_E$  for small values of  $\gamma_E$  [25]. This is despite the fact that both  $v_i$  and  $\chi_i$  individually have strong dependence on  $\kappa$  and  $\gamma_E$ . For  $\gamma_E \geq 0.4$  the Prandtl number is close to unity, in good agreement with experimental measurements at low Mach numbers [27].

*Stiff transport.*—A serious impediment to confinement is the strong sensitivity of the heat flux to small changes in  $\kappa$ . This stiffness of the transport makes it difficult to increase  $\kappa$ , and therefore the core temperature, beyond the critical value,  $\kappa_c$ , at which turbulence is excited. Recent experimental results indicate that the stiffness,  $\partial Q_i/\partial \kappa$ , may be reduced at low magnetic shear and large values of  $\gamma_E$  [12]. For the Cyclone base case considered here ( $\hat{s} = 0.8$ ), we find a complicated dependence of stiffness on flow shear, shown in Fig. 5. At low values of  $\gamma_E$  ( $\leq 0.3$ ), the critical  $\kappa$  shifts to higher values, but the stiffness increases. For  $\kappa/\gamma_E \rightarrow \infty$ , the heat flux tends to the curve corresponding to  $\gamma_E = 0$ ; since  $\kappa_c$  increases with  $\gamma_E$ , the average value of  $\partial Q_i/\partial \kappa$  increases with  $\gamma_E$ .

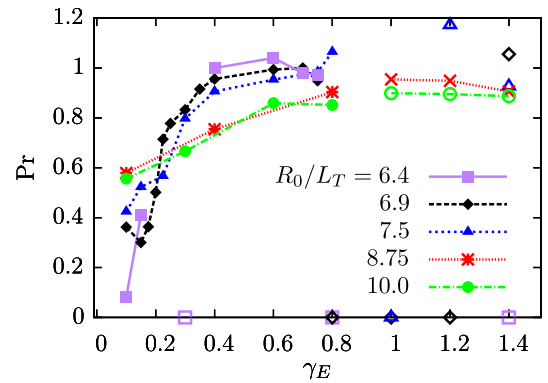


FIG. 4 (color online). Turbulent Prandtl number as a function of flow shear for a range of  $R_0/L_T$  values. Unfilled points correspond to linearly stable flow shear values. Zero  $Pr$  points represent fully suppressed turbulence.

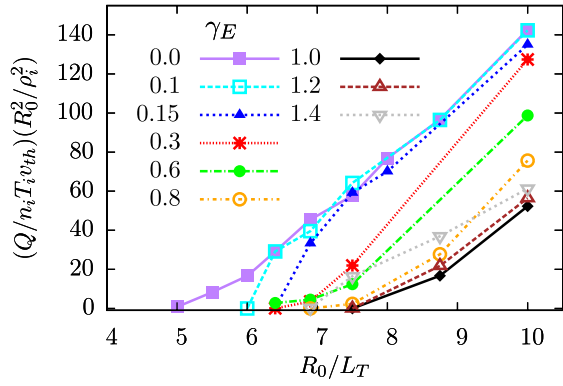


FIG. 5 (color online). Turbulent heat flux vs  $R_0/L_T$  for various values of the flow shear. Though there is some minimal relaxation of the profile stiffness for  $0.3 \lesssim \gamma_E \lesssim 0.8$ , the predominant effect of the shear is to shift the critical temperature gradient.

For  $0.3 \lesssim \gamma_E < \gamma_{Ec}$ , both  $\kappa_c$  and the profile stiffness decrease. This is a result of the change in nature of the linear instability, which is now driven by the PVG. The relaxation of stiffness is modest, and it only occurs for  $\kappa$  near  $\kappa_c$ . When  $\gamma_E > \gamma_{Ec}$ ,  $\kappa_c$  initially shifts upwards with increasing  $\gamma_E$ , and stiffness increases for  $\kappa$  near  $\kappa_c$ . However, for even larger  $\gamma_E$ , both the stiffness and  $\kappa_c$  decrease. This is to be expected, as the subcritical turbulence is driven by the velocity, not temperature, gradient and thus has a weaker dependence on  $\kappa$ . Finally, Fig. 5 shows that, for the parameters considered here,  $\gamma_E = 1$  is the overall optimal value of flow shear, for which any given input  $Q$  results in the largest possible  $\kappa$ .

*Conclusions.*—We have shown that PVG-driven turbulence exists at large flow shears, but only if the initial fluctuation amplitudes are sufficiently large. This has a number of potentially important implications. First, it indicates that linear stability analysis is insufficient to determine critical gradients in rotating plasmas. It also implies the existence of an optimal flow shear for confinement corresponding to each temperature gradient. Furthermore, it shows that the system can undergo hysteresis: an equilibrium state with large flow shear and temperature gradient (e.g.,  $\gamma_E = 1$  and  $R_0/L_T = 10$ ) has large turbulent fluxes if the temperature gradient is obtained at low flow shear, where fluctuations grow due to linear instability and are maintained by subcritical turbulence drive when flow shear is increased. If a large flow shear is obtained before increasing the temperature gradient, then the initial fluctuation amplitudes will not be large enough to achieve subcritical turbulence. In experiment a certain heat flux is maintained via external sources, so the only way to maintain the quiescent solution is for the temperature gradient to get sufficiently large that the heat flux is collisional.

The existence of local maxima of the toroidal angular momentum flux provides the potential for bifurcations in  $\gamma_E$  [28] and corresponding bifurcations in temperature gradient. However, a detailed transport analysis is neces-

sary to study such a bifurcation for experimentally relevant conditions [29]. Finally, because the ratio of the  $\mathbf{E} \times \mathbf{B}$  suppression and PVG drive term is proportional to  $(qR_0/r)$  [9], our results, which should be qualitatively robust, may undergo considerable quantitative variation with changes in magnetic configuration.

The authors are grateful to I. G. Abel, F. J. Casson, W. Dorland, G. W. Hammett, and A. Zocco for useful discussions; they thank the Leverhulme Trust (UK) International Network for Magnetized Plasma Turbulence for travel support. Computing time was provided by EPSRC Grant No. EP/H002081/1.

\*michael.barnes@physics.ox.ac.uk

- [1] K. H. Burrell, *Phys. Plasmas* **4**, 1499 (1997).
- [2] G. D. Conway *et al.*, *Phys. Rev. Lett.* **84**, 1463 (2000).
- [3] G. Tresset *et al.*, *Nucl. Fusion* **42**, 520 (2002).
- [4] A. M. Dimits *et al.*, *Phys. Rev. Lett.* **77**, 71 (1996).
- [5] R. E. Waltz *et al.*, *Phys. Plasmas* **5**, 1784 (1998).
- [6] J. E. Kinsey *et al.*, *Phys. Plasmas* **12**, 062 302 (2005).
- [7] A. G. Peeters and C. Angioni, *Phys. Plasmas* **12**, 072 515 (2005).
- [8] F. J. Casson *et al.*, *Phys. Plasmas* **16**, 092 303 (2009).
- [9] C. M. Roach *et al.*, *Plasma Phys. Controlled Fusion* **51**, 124 020 (2009).
- [10] P. J. Catto *et al.*, *Phys. Fluids* **16**, 1719 (1973).
- [11] P. C. de Vries *et al.*, *Nucl. Fusion* **49**, 075 007 (2009).
- [12] P. Mantica *et al.*, *Phys. Rev. Lett.* **102**, 175002 (2009).
- [13] H. Sugama and W. Horton, *Phys. Plasmas* **4**, 405 (1997).
- [14] I. G. Abel *et al.* (to be published).
- [15] G. W. Hammett *et al.*, *Plasma Phys. Controlled Fusion* **35**, 973 (1993).
- [16] M. Artun and W. M. Tang, *Phys. Plasmas* **1**, 2682 (1994).
- [17] F. L. Hinton and S. K. Wong, *Phys. Fluids* **28**, 3082 (1985).
- [18] M. Kotschenreuther *et al.*, *Comput. Phys. Commun.* **88**, 128 (1995).
- [19] A. M. Dimits *et al.*, *Phys. Plasmas* **7**, 969 (2000).
- [20] F. L. Waelbroeck and L. Chen, *Phys. Fluids B* **3**, 601 (1991).
- [21] S. L. Newton *et al.*, *Plasma Phys. Controlled Fusion* **52**, 125 001 (2010).
- [22] We have verified that this subcritical turbulence persists when kinetic electrons are included, in contrast with the qualitatively different phenomenon observed in [6].
- [23] L. N. Trefethen *et al.*, *Science* **261**, 578 (1993).
- [24] At  $\gamma_E = 0$ ,  $\Pi = 0$  unless up-down asymmetry, the Coriolis drift, or other symmetry-breaking effects are present; A. G. Peeters and C. Angioni, *Phys. Plasmas* **12**, 072 515 (2005); F. I. Parra, M. Barnes, and A. G. Peeters, *Phys. Plasmas* (to be published).
- [25] In [8,26], which consider low flow shear values for which the turbulence is not subcritical, Pr is found to be order unity and independent of  $\gamma_E$  for a single  $\kappa$  value.
- [26] R. E. Waltz *et al.*, *Phys. Plasmas* **14**, 122 507 (2007).
- [27] P. C. de Vries *et al.*, *Plasma Phys. Controlled Fusion* **52**, 065 004 (2010).
- [28] R. E. Waltz *et al.*, *Phys. Plasmas* **2**, 2408 (1995).
- [29] F. I. Parra *et al.*, *Phys. Rev. Lett.* **106**, 115004 (2011).